Spatio-temporal variability of ocean temperature in the Portugal Current System

Ricardo T. Lemos

Faculdade de Ciências da Universidade de Lisboa, Portugal

Bruno Sansó

Department of Applied Mathematics and Statistics, University of California Santa Cruz, USA

Abstract. A dynamic process convolution model (DPCM) is used to investigate the evolution and spatial distribution of monthly ocean temperature anomalies in the Portugal Current System. The analysis is performed with 20th century standard depth measurements from the National Oceanographic Data Center, ranging from the surface to 500 m depth. The proposed DPCM decomposes the temporal variability into short-term non-linear components and long-term linear trends, with both components varying smoothly across latitude, longitude and depth. An important feature of the DPCM is that it allows the assessment of trend significance without ad hoc corrections, since the residuals are spatially and temporally uncorrelated. In the analyzed period, an overall warming of coastal surface waters off the west Iberian Peninsula is found, together with fading cross-shelf temperature gradients and increased coastal stratification. Since previous studies also found that upwelling-favorable winds have weakened from the 1940s onward, these results most likely reflect a long-term weakening of the coastal upwelling regime. Transient periods of temperature change are also described and associated with known variability in the North Atlantic, and a final discussion on the link between the observed trends and anthropogenic forcing on climate is presented.

1. Introduction

Located off the west Iberian Peninsula, the Portugal Current System (PCS) marks the northern extent of the Canary Current System. Analyzes of in-situ measurements and satellite images from the past decades [e.g., *Fiúza*, 1982, 1983, 1984; *Coste et al.*, 1986; *Sousa*, 1995; *Smyth et al.*, 2001; *Martins et al.*, 2002] have revealed the hydrology of this region and showed its geostrophic circulation to include a complex interaction between underlying water masses as well as meteorological conditions. Of particular importance, episodes of upwelling induced by northerly trade winds fuel a rich and diverse ecosystem that is heavily fished. Recent studies have indicated that the upwelling regime in the PCS underwent significant changes between 1941 and 2000 [*Dias*, 1994; *Pires and Antunes*, 2000; *Lemos and Pires*, 2004]. Using coastal wind data, *Lemos and Pires* [2004] found that northerly winds steadily weakened since the 1940s across the west Portuguese coast, especially during the upwelling season (April through September); at the same time, coastal sea-surface temperature (SST) increased at a rate of $1\,^{\circ}\mathrm{C}(100\mathrm{yr})^{-1}$, which was nearly five times higher than in open ocean regions. Since this study was performed using linear regression models, with time as the single predictor variable, relevant spatial and short-term temporal dependencies in the data were not accounted for, which to some degree impaired the assessment of significance in these trends. Hence it was concluded that although the analyzes of wind and SST clearly pointed to a weakening of the PCS seasonal upwelling regime, more elaborate models could be designed to provide a better description of this phenomenon.

In the present paper, an attempt is made to analyze the evolution of ocean temperature anomalies with a statistical model that can deal with spatial and temporal correlations while extracting long-term temporal components. Although more complex than the linear regression model used by *Lemos and Pires* [2004], the model is still simple enough to be fitted with a fast statistical method that can cope with large amounts of data. This feature is taken advantage of, by modeling not only SST but also subsurface temperature, down to 500 m depth. The choice of temperature anomalies over temperature means lies in the fact that anomalies display weaker spatial and temporal variability, hence being easier to model. Also, this enables the analysis to focus mainly on interannual variability. As a disadvantage, possible changes in the amplitude and phase of the yearly cycle of temperature variation cannot be modeled explicitly, the same being true for the depth and strength of the thermocline. Nevertheless, some information about these features may be extracted from the model, as will be shown.

This paper is organized as follows: Section 2 describes the data source and introduces the statistical model used; Section 3 presents the results, together with an evaluation of the model's goodness-of-fit; Section 4 includes an interpretation of the results and a general discussion on fitting trends to environmental data; Section 5 contains some final comments on the usefulness of the statistical methodology developed here and considers the potential link between the observed long-term changes and greenhouse warming.

2. Data and Methodology

2.1. Data

For the region of interest presented in Figure 1, nearly 260 000 monthly 1/4°grid ocean temperature means at 14 standard depths (0, 10, 20, 30, 50, 75, 100, 125, 150, 200, 250, 300, 400 and 500 m) were computed from World Ocean Database 2001 [*Conkright et al.*, 2002] records between Jan-1901 and Dec-2000. Data from all instrument types were used without discrimination. After removing outliers (land

0148-0227/05/$9.00

observations and values exceeding 4 standard deviations from 4° grid monthly fields), anomalies were derived using monthly 1/4° grid climatological mean fields from the World Ocean Atlas 2001 [*Stephens et al.*, 2002]. No smoothing was applied in any of the above steps.

2.2. The Discrete Process Convolution Model

For any given month, ocean temperature anomalies can be seen conceptually as forming a spatially continuous Gaussian random field over a three-dimensional region $D^3 \subset \mathbb{R}^3$. Process convolutions [*Higdon*, 2002], also known as general linear processes [*Priestley*, 1981], provide simple representations of such fields by convolving continuous white noise with a kernel, whose shape determines the covariance structure of the resulting process. This approach is an alternative to traditional geostatistical techniques, where a covariance function is specified directly, but allows for increased flexibility, since the choice of the kernel also allows for features such as non-stationarity, anisotropy, and edge effects [*Calder*, 2003].

A discrete approximation to the process convolution is obtained by letting L^3 be a lattice of n points contained in $\mathbb{R}^3$ (not necessarily in D^3—see *Kern* [2000]), assigning a latent white noise process $x(s)$ to each point $s \in L^3$ and convolving it over D^3 with a three-dimensional smoothing kernel k. Thus, the monthly temperature anomaly at location $l \in D^3$, $Y^{(l)}$, can be approximated by a weighted average of the white noise as

$$Y^{(l)} \approx \sum_{j=1}^{n} \varpi_j x(s_j) = \sum_{j=1}^{n} \frac{k(l-s_j)}{\sum_{i=1}^{n} k(l-s_i)} x(s_j), \qquad (1)$$

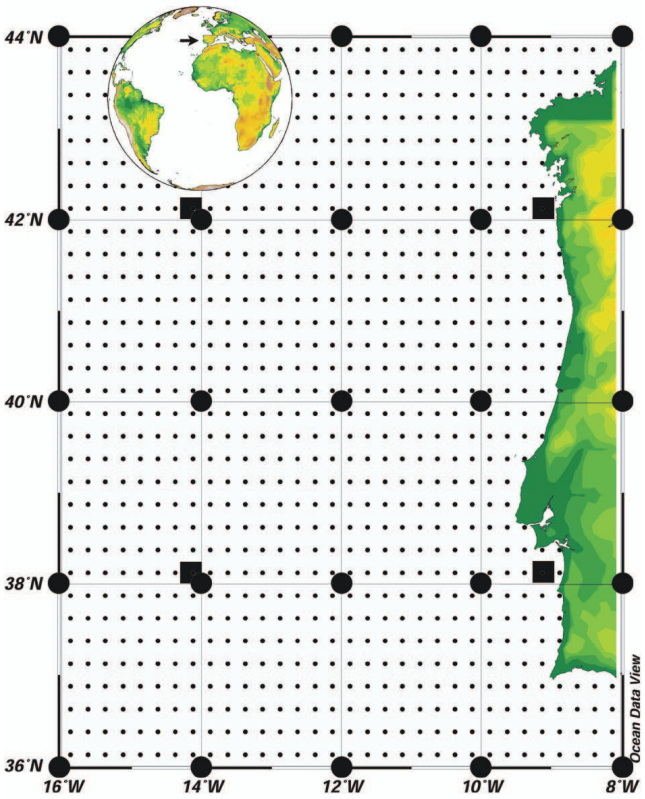

Figure 1. Analyzed region of the Portugal Current System. The 1/4° grid used to compute temperature anomalies is represented by small dots, whereas large dots denote the surface 2° grid lattice. Four squares locate the points where detailed analyzes were performed (see Sections 3.2 and 3.3).

where $k(l - s_\cdot)$ is given by the kernel k centered at point $s_\cdot$ and evaluated at location l. For reasons that will be discussed in Section 2.3, L^3 was defined in the present analysis as a 2° grid with three vertical layers, located at 0, 250 and 500 m, making $n = 75$. A Gaussian kernel was used, with horizontal standard deviation (for latitude/longitude) of 2° and vertical standard deviation (for depth) of 60 m.

As the field of ocean temperature anomalies is expected to change with time, the latent processes are allowed to evolve according to a specified function. The working hypothesis in this paper is that the evolution of temperature anomalies during the 20th century, anywhere in the PCS, may be approximated by a sum of a random walk—termed baseline—and a long-term linear trend. While the former can encompass transient changes in seasonality and average yearly temperature, the latter can accommodate a steady, year-round change of average temperature over the years. Both the baseline and the trend are allowed to change smoothly across space, although at a much faster rate across depth than across latitude or longitude (this can be deducted from the kernel's shape). To account for measurement errors, a third term of white noise is added, producing a Discrete Process Convolution Model (DPCM) that, using vector notation, may be written as

$$\begin{aligned} Y_t &= K_t(\alpha_t + \beta(t - t_R)) + \epsilon_t, \quad \epsilon_t \sim N(0, \sigma^2 I_t), \\ \alpha_t &= \alpha_{t-1} + w_t, \quad w_t \sim N(0, W_t). \end{aligned} \qquad (2)$$

Y_t [°C] is the $q_t \times 1$ vector of q_t observations made in month t, K_t is a unitless $q_t \times n$ convolution matrix containing the weights defined in Equation (1), α_t [°C] and β [°C/month] are $n \times 1$ vectors associated with the baselines and the linear trends, respectively, t_R is an arbitrary time reference, which was set to Dec-2000, ϵ_t [°C] is a $q_t \times 1$ vector of white noise with variance σ^2 [°C^2], I_t is the $q_t \times q_t$ identity matrix, and W_t [°C^2] is a $n \times n$ variance-covariance matrix. To show that Model (2) translates the working hypothesis, consider a single observation made in location l at time t ($q_t = 1, K_t = \varpi'$); then,

$$Y_t^{(l)} \approx \alpha_t^{(l)} + \beta^{(l)}(t - t_R),$$

where $\alpha_t^{(l)} = \varpi'\alpha_t$ and $\beta^{(l)} = \varpi'\beta$ are variables that define, respectively, the ordinate at $t = t_R$ and the slope associated with the trend line at location l. Unlike the slope, the ordinate changes with time, according to the random walk $\alpha_t^{(l)} = \alpha_{t-1}^{(l)} + \varpi' w_t$. Both variables are spatially smooth owing to the $n \times 1$ convolution vector ϖ.

With minor modifications, Model (2) can be represented as a Dynamic Linear Model [DLM; *West and Harrison*, 1997]:

$$\begin{aligned} Y_t &= F_t'\theta_t + \epsilon_t, \quad \epsilon_t \sim N(0, \sigma^2 I_t), \\ \theta_t &= (\alpha_t', \beta_t')' = \theta_{t-1} + w_t, \quad w_t \sim N(0, W_t), \\ \theta_0 &\sim N(m_0, C_0), \end{aligned} \qquad (3)$$

where $F_t' = (K_t, K_t(t - t_R))$ and m_0 and C_0 are the initial priors for the mean and covariance of the $2n \times 1$ vector θ. Within the DLM framework, the unknown evolution variance W_t can be modeled using the discount factor technique and fast, closed form posterior computations can be obtained without resorting to Markov Chain Monte Carlo simulations. A discount factor, say δ, is a number between 0 and 1 that determines the amount of information lost through the process evolution in time. With $\delta = 1$ (no loss) a static model is obtained, whilst small values of δ correspond to heavy discounting of the information available at time $t - 1$. Multi-component models can have different

discount factors for each component [*West and Harrison*, 1997]. In Model (3), the discount factor associated with β_t is set to 1, as this leads to β_t becoming constant over time and capturing the long-term trend of temperature anomalies. To model the evolution variances of α_t, discount factors of 0.995 before Jan-1951 and 0.96 from then onwards were chosen. The former number is a consequence of the extreme sparseness of data until the 1950s, and implies that little variation of the baselines is allowed during the first half of the century. The latter was optimized upon residual analysis (see Section 2.3). It should be pointed out that, like other DLMs, the DPCM can cope with missing data at any time instant t, simply by equaling the posterior distributions to the priors (*West and Harrison* [1997], section 10.5). Given the lack of prior information, flat initial priors with zero mean were used for the $2n$ parameters (n baselines and n trends) at the beginning of the time series.

2.3. Goodness-of-fit Analysis

Several aspects defined the goodness-of-fit of the DPCM. First, the model was expected to efficiently decompose temperature anomalies into long-term trends and (trendless) baselines. The best way to ensure this, albeit computationally burdensome, would be to define the lattice L^3 as fine as the original data set (i.e., with 14 vertical layers and 1/4° horizontal spacing), since the finest spatial variability in both trends and baselines would be captured by the model. Coarse lattices, on the other hand, have the advantage of allowing fast computations but, in some locations, erroneously imbed part of the long-term signal into the baseline. Thus, a tradeoff between efficiency and speed had to be decided, and the final lattice was defined partly upon the following criterion: in 1000 randomly chosen locations taken at varying depths, only about 5% were allowed to display a least squares trend in the baseline component in absolute value greater than $0.5\,^{\circ}\mathrm{C}(100\mathrm{yr})^{-1}$.

Second, the formulation of the model did not consider the possibility of there being long-term changes in the seasonal pattern of temperature variation, because the trend component was defined as the same for all calendar months. If such changes existed anywhere in the PCS, then the baseline and/or the residuals should be contaminated with 12-month periodic signals. To test this hypothesis, least squares models

$$Z_t = a + b\sin(\pi t/6) + c\cos(\pi t/6) + \xi_t \qquad (4)$$

were fitted to the 1000 locations mentioned above. Z_t are either the baseline estimates or the residuals. To safeguard against mistakenly rejecting the null hypothesis that there are no oscillations as a consequence of performing multiple tests, the False Discovery Rate (FDR) routine developed by *Ventura et al.* [2004] was used, with the allowed rate of false rejections out of all rejections equal to 5%. According to these authors, the FDR procedure of *Benjamini and Hochberg* [1995] is robust in situations of spatially correlated data and controls the expected proportion of false rejections better than traditional uncorrected and Bonferroni procedures.

Third, the residuals were expected not to have any spatial or temporal structure. The size of the lattice grid is also important here, since it defines the smallest resolution of spatial features present in the data that can be captured by the model. Thus, to warrant spatially uncorrelated residuals, the lattice should be as fine as the original data set. However, fine lattice DPCMs are more data demanding, because more parameters are being estimated, and cannot cope with many consecutive time instants with few or no observations. Apart from making the grid coarser, the only way to deal with data shortcomings is to increase the discount factor, meaning less new information is being required at each time instant. This latter choice, however, also leads to greater residual correlations, since the model loses some ability to integrate short-scale spatial and temporal features. Hence, several combinations of lattices — with different horizontal spacings, different number of vertical layers and different positions in space —, kernel standard deviations and discount factors were experimented, using as a second criterion the minimization of significant spatial and temporal residual correlations. These where inspected separately, by means of spatial correlograms for synchronous residuals and temporal correlograms for isotopic residuals.

Finally, under the DPCM the residuals were assumed to have asymptotical normal distribution. To investigate this, a "leave one out" cross-validation was performed by producing a qq-plot of standardized residuals from 200 randomly selected observations from each decade of the 20th century. If the assumption was correct, standardized residuals should have asymptotical standard normal distribution.

3. Results

3.1. Long-term Trend Estimates

Figure 2 depicts the spatial variation of long-term linear trends found in temperature anomalies of the PCS, at four depths. The trends and respective 95% posterior intervals were estimated at points located on the 1/4° grid shown in Figure 1 and then interpolated using the VG gridding option of the software Ocean Data View [*Schlitzer*, 2003], with just enough smoothing (5% of the axes length) to create a continuous surface. Since the spatial variation of trends was modeled as a continuous process, the grid size could have been decreased indefinitely to obtain more accurate contours.

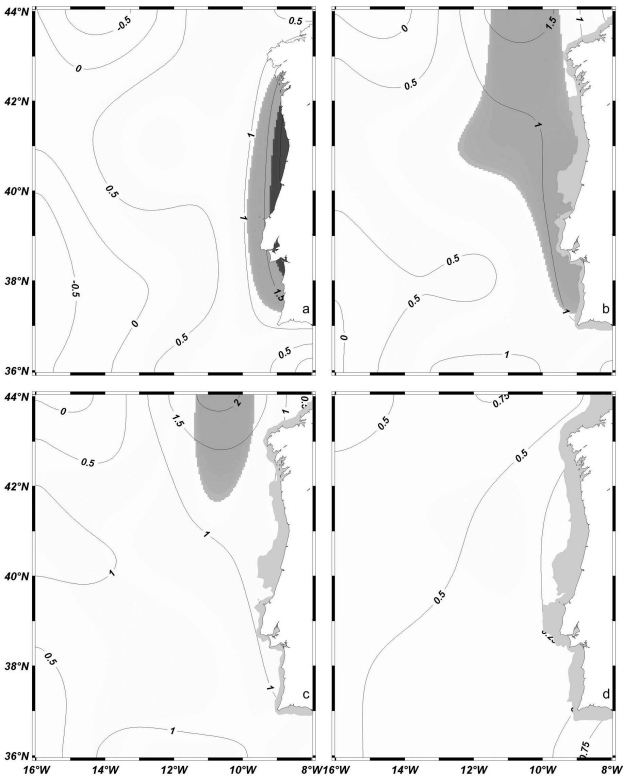

Figure 2. Long-term trend estimates [$^{\circ}\mathrm{C}(100\mathrm{yr})^{-1}$] at (a) 0 m, (b) 150 m, (c) 200 m, (d) 500 m. Intermediate and dark gray regions have 95% posterior intervals above 0 and $0.5\,^{\circ}\mathrm{C}(100\mathrm{yr})^{-1}$, respectively. Light gray regions are shallower than the depth analyzed.

At the sea surface (Figure 2a), the presence of positive trends with high, significant values close to the west Iberian coast is noteworthy. The area with significant trends increases with depth and reaches its maximum extent at 150 m (Figure 2b). At this depth, the area where trends exceed $1\,^{\circ}\mathrm{C}(100\mathrm{yr})^{-1}$ is also greater than at 0 m, and continues to grow down to 200 m, where negative trends have almost disappeared (Figure 2c). Further down, trends are everywhere positive but non-significant (Figure 2d).

3.2. Baseline Estimates

Figure 3 shows time series plots of baseline estimates at two coastal and two offshore locations. Several interesting features are revealed. Firstly, the sparseness of available data for the first half of the 20th century leads to wide posterior bands and renders short scale spatio-temporal variability undetectable in this period. Nevertheless, wide variations of the surface baseline are apparent between 1920 and 1950 and a synchronized fluctuation is discernible, with maxima in the late 1920s and 1940s and minima in the early 1920s and mid 1930s. This fluctuation is stronger in coastal regions of the PCS and is dampened with depth, becoming indistinguishable at 200 m.

Secondly, the post-1950 interannual and interdecadal evolution of the baselines is very similar at distant locations in the PCS, when taking into consideration the uncertainty associated with the estimates. Until the early 1970s, a pronounced cooling that began in the 1940s is evident. Afterwards, a sustained warming that lasts until the end of the time series is observed.

To better detail the spatial variability of these episodes of temperature change, 5-year means of the baseline were computed for 1951-1955, 1971-1975 and 1996-2000. The differences between these means at 0 and 300 m are presented in Figure 4; 95% posterior intervals for these differences were produced by obtaining 5000 samples from the joint posterior. At the surface, the baselines decreased significantly from the 1950s to the 1970s almost everywhere in the PCS, exceeding a difference of $-1\,^{\circ}\mathrm{C}$ between 12 and 15°W. This process of cooling associated with the baselines is still detectable at 300 m, but only in offshore regions. When comparing the 1950s with the 1990s, the latter period has warmer waters in the upper 125 m and cooler offshore waters down to 500 m, but the regions where significant changes in the baselines exist are few; also, no large scale meridional or zonal gradients are evident. Thus, in terms of the baselines, the early 1950s and the late 1990s may be considered alike.

3.3. Temperature estimates

Several results of the DPCM are presented here: first, a reconstruction of the evolution of ocean temperature in

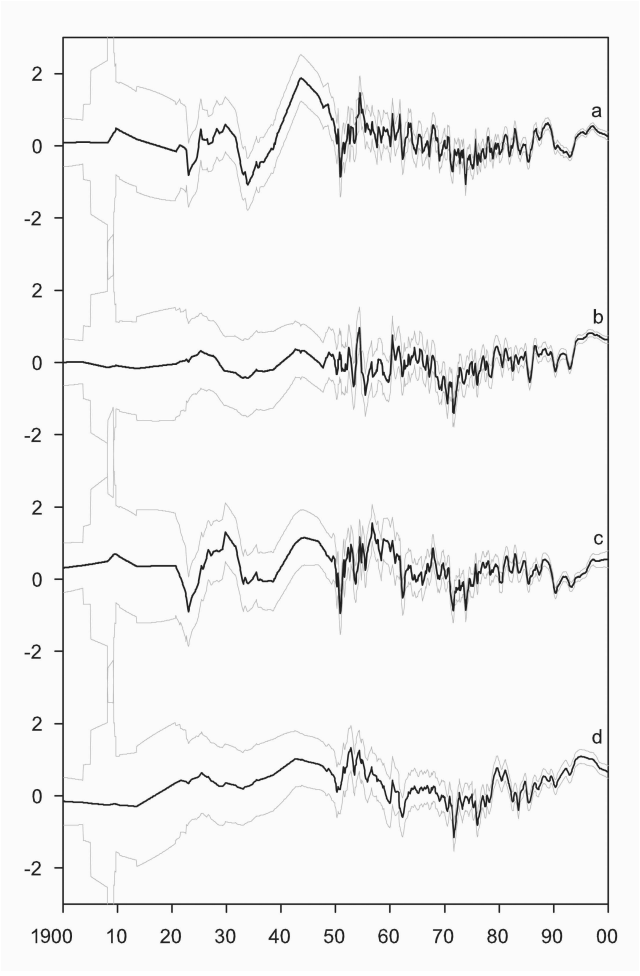

Figure 3. Evolution of monthly sea surface baseline estimates [°C] at (a) 38.125°N, 9.125°W; (b) 38.125°N, 14.125°W; (c) 42.125°N, 9.125°W; (d) 42.125°N, 14.125°W. 95% posterior bands are drawn in gray.

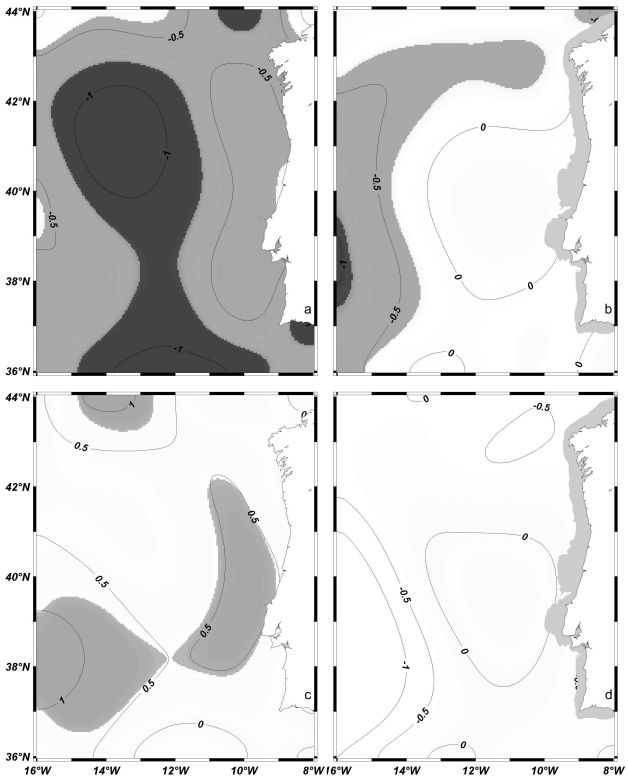

Figure 4. (a) The difference [°C] between monthly sea surface baselines averaged from 1971 to 1975 and monthly sea surface baselines averaged from 1951 to 1955. Intermediate and dark gray regions have 95% posterior intervals below 0 and -0.5°C, respectively. (b) As in (a) but for 300 m depth. (c) Difference between monthly sea surface baselines averaged from 1996 to 2000 and averaged from 1951 to 1955. Intermediate and dark gray regions have 95% posterior intervals above 0 and 0.5°C, respectively. (d) As in (c) but for 300 m depth.

a coastal location, depicting both short- and long-term changes; second, surface plots of temperature differences between the periods considered in Section 3.2; third, time series plots of temperature differences between coastal and offshore locations; finally, two surface plots showing the evolution of upper ocean stability during summer, in two cross-shore sections off the west Iberian coast.

3.3.1. Coastal temperature change

During the data rich period of 1981–2000, observations in the PCS are available nearly every month, allowing the DPCM to produce narrow 95% posterior intervals for the mean and hence enabling the detection of significant short-term temperature changes. For instance, Figure 5 shows that between 1981 and 1995, mean SST anomalies in the SW Iberian coast fluctuated around 0°C, whilst from then onwards they remained positive. Given the final estimate of error variance, $\sigma^2 = 0.28°C^2$, 95% posterior intervals for the observations (which include the uncertainty related to the mean) have in this case a range close to 3°C.

In other periods, fewer measurements are available and the DPCM performs poorer, making the study of interannual temperature changes more interesting. Following the previous example, Figure 6 displays a profile on the evolution of annual temperature off SW Iberia. The long-term increase of temperature differences between surface and subsurface waters, due to the significant warming of the former, is remarkable. Also, the early onset of subsurface (< 125 m) temperature warming in the late 1960s can be discerned. A third interesting feature is the dampening of interannual temperature variability with depth. For reasons of clarity, posterior intervals were not depicted along with the average estimates; these would have shown the great uncertainty related to temperature change prior to 1950.

3.3.2. Periods of cooling and warming

The 3 periods considered in Section 3.2 are again compared in Figure 7, but the impact of long-term trends is now included. Thus, differences between 5-year means of temperature anomalies are portrayed. As Figure 7a shows, coastal surface waters off Iberia remained at a nearly constant temperature from the early 1950s to the 1970s, instead of cooling along with offshore waters. If this figure is compared with Figure 4, it may be deduced that the distinct behavior of coastal and offshore waters is in part due to the long-term warming of the former. At 300 m, the cooling associated with the baselines (Figure 4b) is counterweighted by the trends (Figure 7b). Thus, only offshore waters of the PCS above 300 m underwent a significant change in ocean temperature.

When the early 1950s are compared with the late 1990s the results are almost symmetrical. In terms of the baselines, it had been shown that the two periods were similar in the upper 300 m (Figures 4c and d). However, when trends are included, a significant surface warming from the former to the later period is found east of 12°W, being stronger in coastal waters (Figure 7c); at 300 m, the impact of the

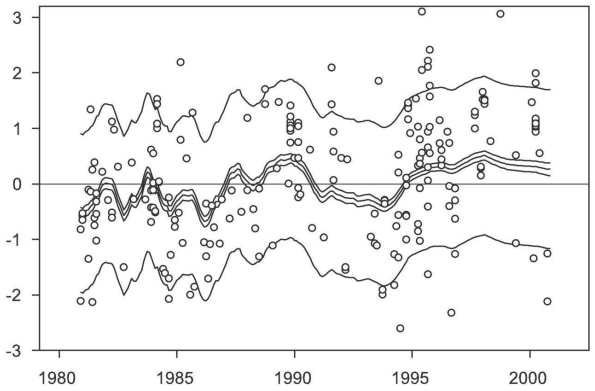

Figure 5. Monthly estimates [°C] of mean SST anomaly (central curve) and 95% posterior intervals for the mean (inner band) and for the observations (outer band) at (38.125°N, 9.125°W), along with observations made in a 1° square centered on that point.

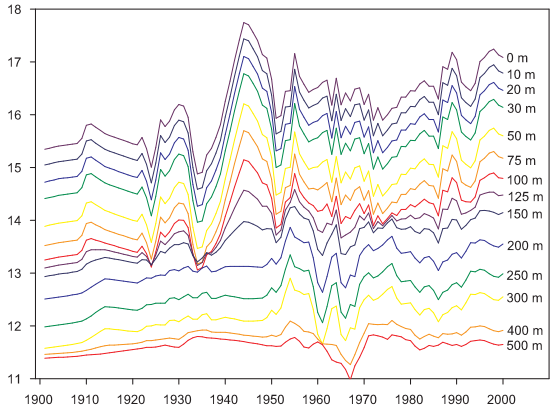

Figure 6. Evolution of annual temperature [°C] at (38.125°N, 9.125°W).

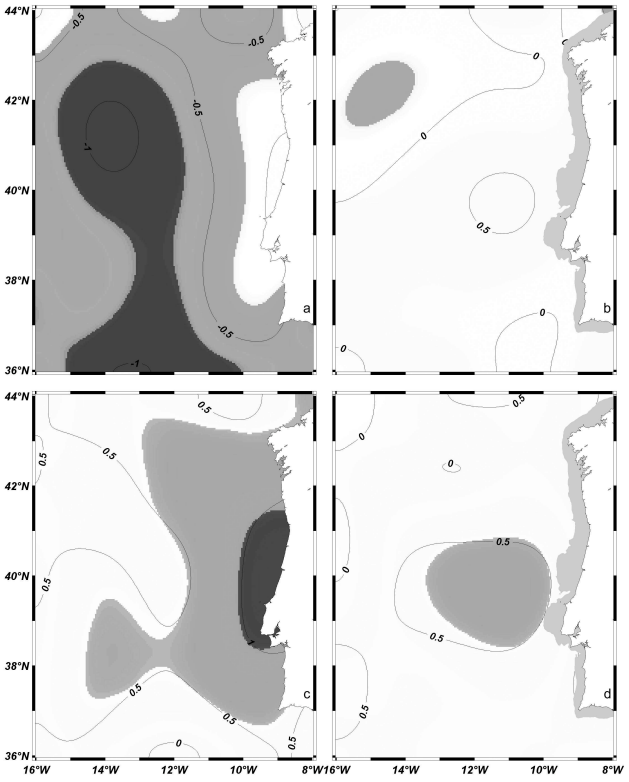

Figure 7. As in Figure 4 but for temperature anomaly estimates obtained as baselines plus long-term trends.

trends is smaller but still introduces significant differences at mid-latitude (Figure 7d).

3.3.3. Longitudinal temperature gradients

Previous results have shown that both trends and baselines have greater zonal than meridional variability (Figures 2, 4 and 7). Hence, temperature gradients in the longitudinal axis are likely to have changed significantly throughout the 20th century, while remaining more or less stable in the latitudinal axis. To inspect this, differences between coastal (9.125°W) and offshore (14.125°W) annual average temperatures at 100 m depth intervals were computed for two latitudes (38.125°N and 42.125°N) and plotted in Figure 8. At both latitudes, the long-term weakening of temperature gradients at all depths is remarkable. The rate of gradient change appears to increase with increasing initial gradient and has a negative sign below 300 m, where cooler waters are present offshore. When compared, gradients off NW and SW Iberia also display similar short-term fluctuations in terms of timing and amplitude, pointing to the stability of meridional gradients. There are, however, some important differences. Off SW Iberia (Figure 8a), gradients in the upper 100 m changed markedly prior to 1950 and stabilized from then onwards at negative values; at greater depths, the convergence to 0°C proceeded until 2000 but was not reached. In contrast, off the NW coast (Figure 8b), the rate of change in the upper layer was small but steady, and subsurface 0°C average annual gradients were reached before the end of the time series.

3.3.4. Upper ocean stability

Stability in the upper layer of the ocean is primarily determined by a balance between the net downward heat flux across the air-sea interface and turbulent mixing processes associated with wind stirring and convective cooling [*Husby and Nelson*, 1982]. In summer months, the outcome of this balance in the PCS is generally in favor of stratification of offshore waters, and some mixing of coastal waters due to upwelling-favorable winds.

To analyze the evolution of upper ocean stability during summer, the climatological temperature fields produced by *Stephens et al.* [2002] were added to anomaly fields resulting from the DPCM, thus yielding monthly vertical temperature profiles on a 1/4° grid. From these, temperature gradients between successive standard depths down to 200 m were computed, and the maximum gradient obtained was considered an indicator of water column stability in the upper layer of the ocean (i.e., strong gradients are indicative of stratified water columns). Figure 9 depicts the evolution of this variable across two longitudinal sections in July. During this month, the seasonal thermocline is located above 50 m everywhere (not shown), but its strength varies in space and over the years: while offshore regions present strong vertical temperature gradients and little temporal variability, coastal regions have on average weaker gradients and display important decadal fluctuations, as well as a general trend towards

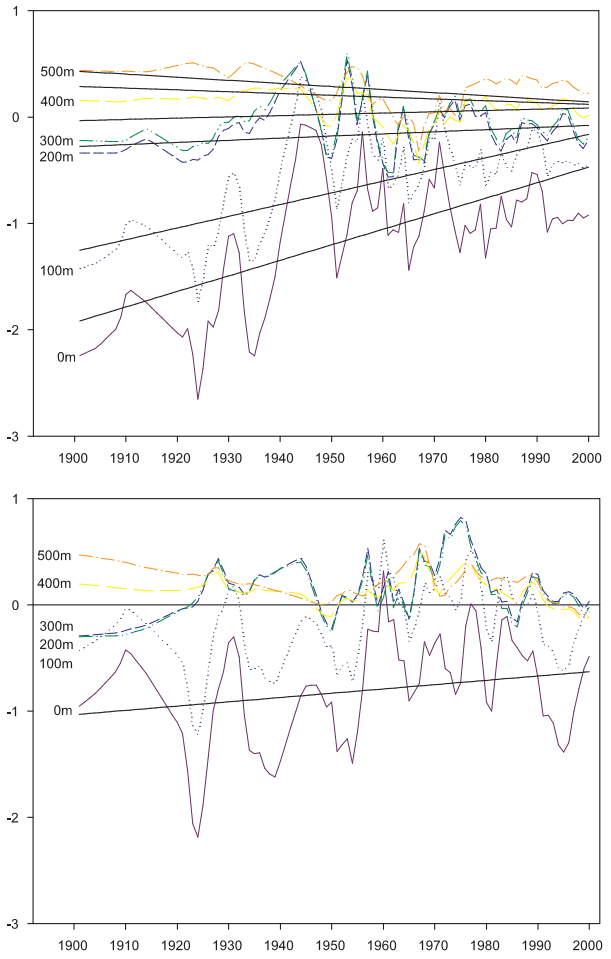

Figure 8. Evolution of annual temperature differences [°C] between 14.125°W and 9.125°W at (a) 38.125°N and (b) 42.125°N. In (a), least squares trend lines were fitted to the curves. In (b), for clarity, the same was performed only for 0 m depth and the 0°C difference line was included.

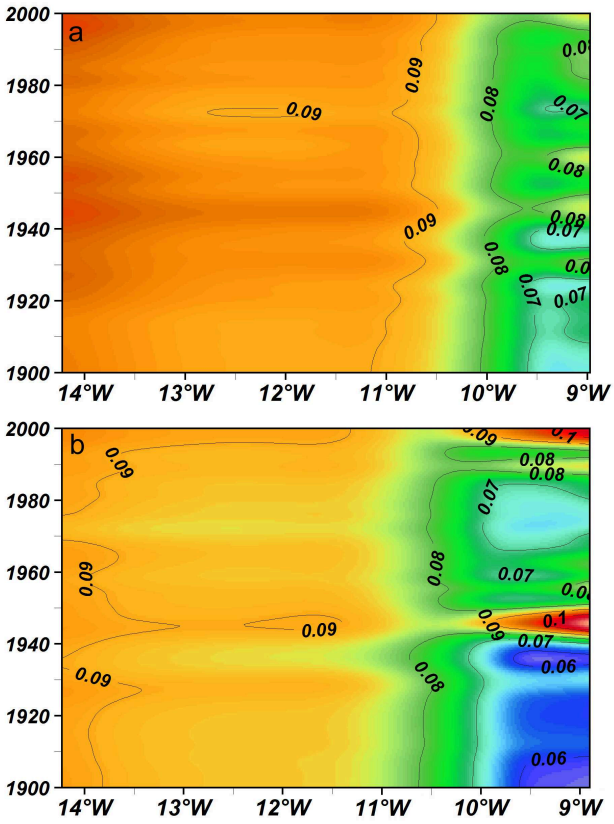

Figure 9. Evolution of July's maximum temperature gradient [°C/m] in the upper ocean layer, in two cross-shelf sections (9 − 14°W): (a) 42.125°N; (b) 38.125°N.

stratification. In Figure 9b, the rapid transition between well-mixed waters and strongly stratified waters is noteworthy.

3.4. Goodness-of-fit Analysis

The lattice L^3 used (with 3 vertical layers and 2° horizontal spacing), along with a time-varying discount factor associated with α_t (equal to 0.995 before Jan-1951 and 0.96 afterwards), produced a fast-running DPCM able to efficiently decompose long- and short-term temperature features in most regions of the PCS. From 1000 randomly chosen sets of coordinates and depths, 80% presented least squares trends fitted to the baselines between -0.25 and 0.25°C(100yr)$^{-1}$, while only 6% exceeded in absolute value 0.5°C(100yr)$^{-1}$. Despite raising some concerns, this latter percentage was considered acceptable, given the simplicity of the model and the multiple constraints provided by the data. The use of a single year-round trend also seemed appropriate, since Model (4) yielded no significant 12-month oscillations in any of the 1000 locations, in both baselines and residuals, when multiple testing was accounted for with the FPR procedure. Of course, this result does not rule out the existence of non-stationary seasonality, since this feature is included in the baseline (see, e.g., Figure 5).

Since clusters of temperature measurements were too infrequent in the analyzed data set, mesoscale oceanic features were impossible to capture with the DPCM. As a consequence, significant spatial correlations with a characteristic exponential-like decay with distance were observed in the residuals (Figure 10a). To mitigate this shortcoming, it should be pointed out that in many cases, synchronous, nearby monthly temperature anomalies were computed with records provided exclusively by the same cruise, making systematic measurement biases another plausible source of residual spatial correlations. In any case, there are indications that the DPCM was able to capture the better part

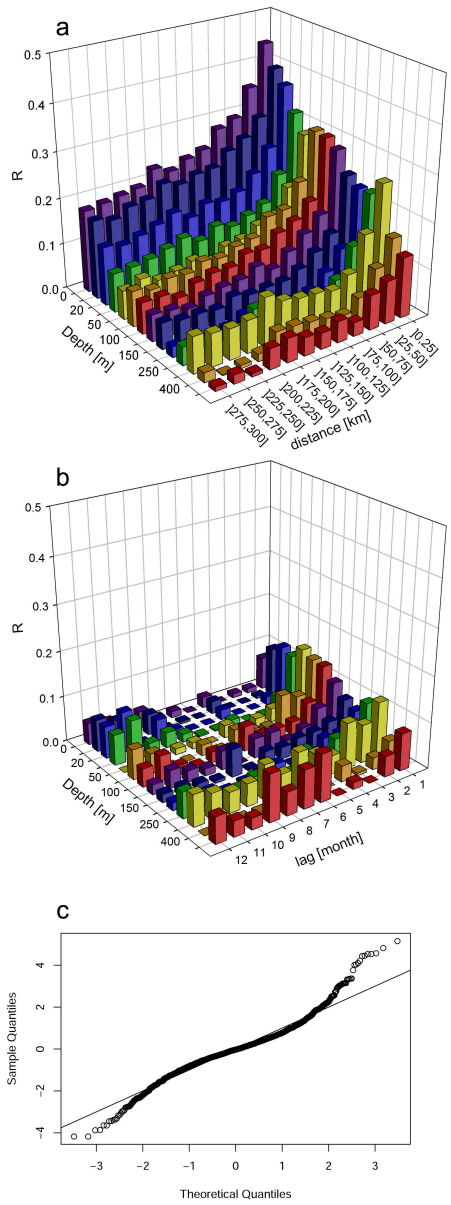

Figure 10. Plots of residuals from the DPCM: (a) Spatial correlation plot; (b) Temporal correlation plot; (c) Quantile-quantile plot of standardized residuals from a "leave one out"cross validation procedure (the expected standard normal distribution is depicted by the line). All the available observations were used to produce the plots in (a) and (b). For clarity, only 2000 observations were used in (c), and negative correlations were not represented in (a) and (b).

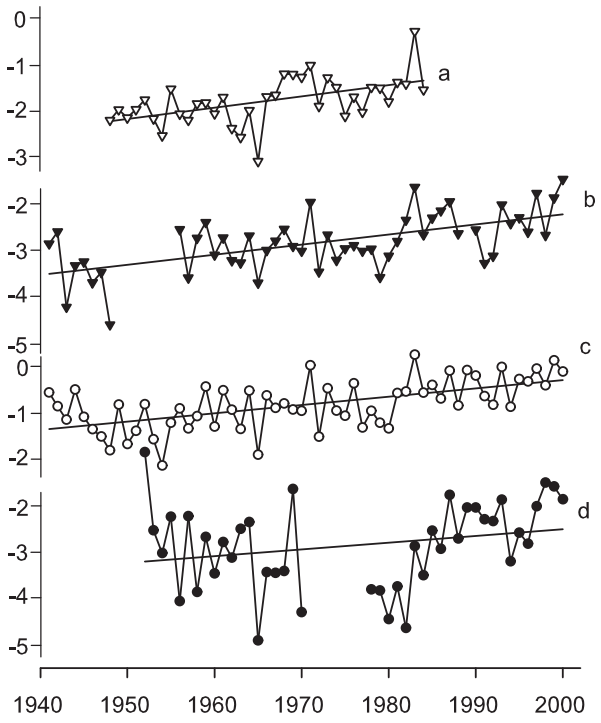

Figure 11. Evolution of the April-September average meridional wind component [m/s] at four coastal weather stations: (a) Porto (41.1°N); (b) Cape Carvoeiro (39.4°N); (c) Lisbon (38.7°N); (d) Sagres (37.0°N). Negative values indicate northerly, upwelling-favorable winds. To point out the similar long-term behavior of the meridional wind component across the western Iberian Peninsula, least squares regression lines were fitted to the data. Data from *Lemos and Pires* [2004].

of spatial temperature variability: when *Lemos and Pires* [2004] applied a linear regression technique to model the evolution of SST in 6 regions of the PCS, roughly 200 km apart, they obtained residuals whose spatial correlation ranged between 0.48 and 0.81; with the present model, the surface residual correlation for a distance of 200 km was close to 0.20.

Unlike the spatial correlation plot, the temporal correlation plot did not present any noticeable residual structure (Figure 10b), meaning the DPCM successfully integrated all the temporal variability of ocean temperature.

Finally, given the large number of observations available, standardized residuals from the "leave one out"cross validation procedure should have standard normal distribution. While there was no overall major violation to this assumption, the tails of the observed distribution were somewhat heavier than expected for a normal (Figure 10c). When qq-plots were produced for each depth fitted separately, the residuals closely followed the best fitting line, whose slope averaged 1 but varied from one plot to another, tending to decrease with depth. Thus, the assumption of normality seemed correct, but considering the error variance not to change with depth was too stringent. To tackle this problem, which does not impair the results presented so far, σ^2 should be replaced either with a parametric function of depth or with a random process. In both cases, the error covariance matrix in Model (3) would change from a multiple of the identity to a diagonal matrix, and Markov Chain Monte Carlo methods would be needed.

4. Discussion

In this paper, the evolution of ocean temperature anomalies in the PCS was modeled as a spatially smoothed sum of a random walk and a linear trend. Although innovative, this technique bears much resemblance to the class of models presented by *Stroud et al.* [2001], where the mean function is written as a time-varying, locally-weighted mixture of linear regressions.

Instead of the century-long trend, a different approach using piecewise linear modeling [*Seidel and Lanzante*, 2004; *Tomé and Miranda*, 2004] might have been attempted; this could have provided further insight in the onset and extent of medium-term (10-50 years) events of temperature change. Or, a non-linear trend might have been fitted, simply by letting the discount factor associated with β_t be less than 1 (see Section 2.2); this would have yielded a model similar to those of Mendelssohn, Schwing and coworkers [*Schwing and Mendelssohn*, 1998; *Schwing et al.*, 1998; *Mendelssohn and Schwing*, 2002; *Mendelssohn et al.*, 2003]. A third possibility would be to use the second order polynomial models described by *West and Harrison* [1997], which provide a local linear trend. However, from the goodness-of-fit analysis performed to the DPCM, there were no indications that making the trend more flexible would have resulted in a better fit—the baseline seemed to be able to encompass all the short- to medium-term variability while leaving temporally uncorrelated observational errors. Hence, the trend was allowed to remain single and linear so as to pursue an important question for climatology: "Were there regions in the PCS where a significant overall change of temperature occurred in the 20th century?".

From the analysis of the World Ocean Database 2001, an interesting answer emerged: overall changes were significant in coastal waters of the PCS, but not in offshore regions (Figure 2). Surface trends were found to vary little with latitude and average $1.2\,^{\circ}\mathrm{C}(100\mathrm{yr})^{-1}$ and $0.2\,^{\circ}\mathrm{C}(100\mathrm{yr})^{-1}$ in coastal ($< 10^{\circ}$W) and offshore (12–15°W) regions, respectively. These estimates closely resemble those obtained by *Lemos and Pires* [2004], who used SST records between 1946 and 1997 from a nearly independent collection, the Comprehensive Ocean-Atmosphere Data Set [COADS; *Woodruff et al.*, 1998]. It should be noted, however, that the results differ in terms of significance, mostly because *Lemos and Pires* [2004] did not insert any spatial or short-term temporal features into their model; when present in the data, these features are known to affect the performance of significance tests (see Section 5).

As a new finding, the present work shows that significant coastal trends range from the surface to 300 m depth; also, the area with significant trends reaches its maximum extent at 150 m, even though the trends are not as strong as at the surface (Figure 2). This higher signal-to-noise ratio present in subsurface waters may be due to their ability to integrate long-term changes in surface fluxes, while changes in surface fluxes themselves may be extremely difficult to measure because of the high level of variability on many timescales [*Banks and Wood*, 2002].

In connection with the observed spatial variability of long-term trends, marked reductions of annual temperature gradients between coastal and offshore regions were found (Figure 8), together with a shallowing of the summer coastal thermocline depth (Figure 9). In a current system such as the PCS, where seasonal episodes of upwelling cool the upper ocean layer (200–300 m) in coastal waters [*Fiúza*, 1984], the aforementioned phenomena may best be explained by a weakening of the upwelling regime, as suggested already by *Dias* [1994] and *Lemos and Pires* [2004]. In these earlier studies, this conclusion partly derived from analyzes of wind records, since a significant, long-term weakening of northerly, upwelling-favorable winds was found across the Portuguese coast (Figure 11).

Although significant linear trends were found in some regions of the PCS, the evolution of temperature anomalies was everywhere far from linear, owing to interdecadal fluctuations of the same magnitude as the trends (Figure 4). Unlike the trends, these fluctuations affected coastal and offshore regions alike and, as will be discussed in the next paragraphs, were closely related to basinwide phenomena.

For the first half of the 20th century, model estimates are associated with wide posterior intervals (Figure 3), meaning there is low certainty regarding the onset, extent and amplitude of temperature changes. Nevertheless, the period of warming that characterized the North Atlantic from the 1920s onward [*Kushnir*, 1994; *Delworth and Knutson*, 2000] may be discerned. In the mid-1920s and 1930s, transient periods of strong upwelling are apparent, especially in the SW Iberian coast (Figures 3 and 8), but this finding should be corroborated with further data.

From the 1950s to the 1970s, the North Atlantic underwent a phase of cooling [*Kushnir*, 1994], and the PCS was no exception (Figure 7a and b). In an analysis of subsurface temperature change between the two decades, *Ezer et al.* [1995] obtained average values close to -0.4°C in the upper 100 m and +0.05°C at greater depths. The surfaces presented in Figure 7 agree with these results but show an important difference between coastal and offshore surface waters, since in the former, the long-term warming trends suppressed the cooling event (see subsection 3.3.2).

From the 1970s to the late 1990s, the short-term variability of ocean temperature in the PCS returned to the levels it had in the early 1950s (Figure 4c and d). This reversal was also observed in SST from other regions of the Canary Current System [*Kifani*, 1998], as well as the NE Atlantic on the whole [*Casey and Cornillon*, 2001, Fig. 3g]. However, when long-term trends were accounted for, coastal regions revealed a marked temperature increase (Figure 7c and d). Again, the long-term weakening of the upwelling regime seems the best candidate to explain this phenomenon.

In conclusion, the temporal variability of ocean temperature in the PCS, during the 20th century, seems to have derived from two major sources: one consisted of well-described, basinwide, short- to medium-term variability; another was identified as a local, long-term weakening of the west Iberian upwelling regime.

5. Concluding Remarks

In climate change research, long-term changes of variables such as ocean and air temperature are frequently investigated. A common approach is to bin the available observations into geographic regions and, separately for each bin, fit a least squares regression model with time as the predictor variable and assess the significance of the obtained slope [e.g. *Casey and Cornillon*, 2001; *Beig et al.*, 2003, and references therein]. Some comments are in order here:

First, due to the common sampling errors in oceanic and atmospheric data sets, adjacent regions may present largely distinct trends. Statistical methodologies that estimate the spatial variation of trends without isolating the bins seem preferable, since they are more resilient to this problem. The usefulness of such methodologies is increased in regions where the analyzed variable presents strong gradients, such as boundary current systems, since the detection of marked spatial variability of trends may be attributed with higher confidence to a long-term change of the physical phenomenon that leads to the observed gradient.

Second, climatic data often present significant spatial and temporal correlations. This impairs the search for long-term changes, because the number of effectively independent observations (n_{eff}) available to standard statistical techniques is smaller than the sample size. The impact of serial correlation is so important that *Santer et al.* [2000] and *Yue et al.* [2002] have shown it to critically affect decisions on the significance of air temperature and river streamflow trends, respectively. The same studies, however, also showed that the various procedures available to account for temporal autocorrelation have differing impacts on trend significance [for another analysis, see *Alpargu and Dutilleul*, 2003]. When analyzing binned data, spatial correlations further reduce n_{eff}, and the way how corrections are made to standard techniques becomes more complicated [see *Yue and Wang*, 2002], especially in the frequent cases where spatial and temporal features cannot be modeled separately. Hence, more complex statistical models that integrate them and do not require post-hoc corrections may in fact provide easier ways to estimate trend significance.

Third, to understand the evolution of a physical property relevant to climate change research, it is also useful to study the way how transient anomalies formed around the trends and how they became distributed in space. Along with the trends, this information is important to assess the quality of numerical models that may be developed to investigate the causes for the observed changes.

In light of the above comments, the statistical methodology developed in this paper seems to present a valuable contribution to climate change research and other types of analyzes where the data present complex features on various spatial and temporal scales.

Together with previous analyzes [*Dias*, 1994; *Lemos and Pires*, 2004], the results presented here point to a significant weakening of the upwelling regime in the PCS. Several questions may have arisen up to this point, namely: What was the extent of the Canary Current System that displayed this behavior? Did other major upwelling regions present similar trends? Was anthropogenic climate change the cause for this phenomenon? What will be the likely response of upwelling systems to future buildup of CO_2 in the atmosphere? Some responses are attempted in these final paragraphs.

Regarding the first two questions, most available information was produced in the Climate and Eastern Ocean Systems Project conference held in 1994, and suggested an intensification of upwelling off NW Africa [*Binet et al.*, 1998; *Demarcq*, 1998; *Kifani*, 1998], with an intriguing blend of stronger equatorward (upwelling-favorable) winds and warmer coastal SST being found in southernmost regions [*Roy and Mendelssohn*, 1998]. The resulting meridional pattern of trends for the whole Canary Current System—including weaker upwelling winds and warmer SST in the northern extent—thus resembles the one found by *Schwing et al.* [1998] in the California Current System (CCS). However, as *Roy and Mendelssohn* [1998] pointed out, trends computed with different data sets displayed inconsistencies, and important biases in COADS data must be sorted out to avoid erroneous interpretations.

More recently, *Mendelssohn et al.* [2003] modeled surface and subsurface temperature data from the CCS with a state-space model, and found that the first two common trends displayed a warming tendency. In all locations surveyed, the first common trend had positive loadings whose amplitude decreased with depth, indicating that the mean temperature of the upper ocean layer increased during the period analyzed (1950-1993). The second common trend, which accounted for much of the remaining variability, had positive loadings in coastal regions and negative loadings in offshore regions, thereby enhancing the warming tendency in the former and mitigating it in the latter. The resulting pattern of long-term change is thus identical to that described in the present paper, which is an interesting finding since the PCS and the CCS are located at the same latitude, albeit in different oceans. Added to this, the most important decadal fluctuations of ocean temperature also seem to be synchronized between current systems (cf. Figure 7 of *Mendelssohn et al.* [2003] with Figure 6).

The latter two questions are also delicate to answer, because opposing viewpoints exist on the implications of greenhouse warming to coastal upwelling systems. According to one [*Bakun*, 1990], increased greenhouse effects may enhance temperature gradients between the oceans and the continents, which in turn strengthen alongshore winds and thus coastal upwelling. According to another [*Wright et al.*, 1986; *Kennedy et al.*, 2002], weaker upwelling may result from a combination of the following phenomena: greater surface heating, reduced salinity of surface waters, and weaker winds produced by smaller thermal gradients between polar and equatorial regions. So far, different climate models have provided responses that support either view as well as neither one [cf. *Bopp et al.*, 2001; *Mote and Mantua*, 2002; *Snyder et al.*, 2003]. In conclusion, the subject of local and global changes in upwelling systems still presents important challenges to be investigated in future work.

Acknowledgments. The authors thank two anonymous reviewers for their comments on an earlier draft of this article, and Roy Mendelssohn for a fruitful discussion concerning the DPCM and its results. The first author acknowledges a scholarship from FLAD (Luso-American Development Foundation).

References

Alpargu, G., and P. Dutilleul (2003), To be or not to be valid in testing the significance of the slope in simple quantitative linear models with autocorrelated errors, *Journal of Statistical Computation and Simulation*, *73*(3), 165–180.

Bakun, A. (1990), Global climate change and intensification of coastal upwelling, *Science*, *247*, 198–201.

Banks, H., and R. Wood (2002), Where to look for anthropogenic climate change in the ocean, *Journal of Climate*, *15*(8), 879–891.

Beig, G., P. Keckhut, R. P. Lowe, R. G. Roble, M. G. Mlynczak, J. Scheer, V. I. Fomichev, D. Offermann, W. J. R. French, M. G. Shepherd, A. I. Semenov, E. E. Remsberg, C. Y. She, F. J. Lbken, J. Bremer, B. R. Clemesha, J. Stegman, F. Sigernes, and S. Fadnavis (2003), Review of mesospheric temperature trends, *Reviews of Geophysics*, *41*(4), 1015, doi:10.1029/2002RG000,121.

Benjamini, Y., and Y. Hochberg (1995), Controlling the false discovery rate: a practical and powerful approach to multiple testing, *J. Roy. Stat. Soc. B*, *57*, 289–300.

Binet, D., B. Samb, M. T. Sidi, J.-J. Levenez, and J. Servain (1998), Sardine and other pelagic fisheries changes associated with multi-year trade wind increases in the Southern Canary Current, in *Global versus local changes in upwelling systems*, edited by M.-H. Durand, P. Cury, R. Mendelssohn, C. Roy, A. Bakun, and D. Pauly, pp. 211–233, ORSTOM.

Bopp, L., P. Monfray, O. Aumont, J.-L. Dufresne, H. LeTreut, G. Madec, L. Terray, and J. C. Orr (2001), Potential impact of climate change on marine export production, *Glob. Biogeochem. Cyc.*, *15*, 81–99.

Calder, C. A. (2003), Exploring latent structure in spatial temporal processes using process convolutions, Ph.D. thesis, Duke University.

Casey, K. S., and P. Cornillon (2001), Global and regional sea surface temperature trends, *Journal of Climate*, *14*(18), 3801–3818.

Conkright, M. E., J. I. Antonov, O. Baranova, T. P. Boyer, H. E. Garcia, R. Gelfeld, D. Johnson, R. A. Locarnini, P. P. Murphy, T. D. O'Brien, I. Smolyar, and C. Stephens (2002), *NOAA Atlas NESDIS 42, World Ocean Database 2001 Volume 1: Introduction*, U.S. Gov. Printing Office, Wash., D.C.

Coste, B., A. Fiúza, and H. Minas (1986), Conditions hydrologiques et chimiques associées à l'upwelling côtier du Portugal en fin d'été, *Oceanologica Acta*, *9*(2), 149–158.

Delworth, T. L., and T. R. Knutson (2000), Simulation of early 20th century global warming, *Science*, *287*(5461), 2246–2250.

Demarcq, H. (1998), Spatial and temporal dynamics of the upwelling system off Senegal and Mauritania: local change and trend, in *Global versus local changes in upwelling systems*, edited by M.-H. Durand, P. Cury, R. Mendelssohn, C. Roy, A. Bakun, and D. Pauly, pp. 149–165, ORSTOM.

Dias, C. M. A. (1994), Notas sobre o hidroclima costeiro de Portugal continental [Notes on the Portuguese continental coast hydroclimate], *internal report*, IPIMAR, Lisbon.

Ezer, T., G. L. Mellor, and R. J. Greatbatch (1995), On the interpentadal variability of the North Atlantic Ocean: model simulated changes in transport, meridional heat flux and coastal sea level between 1955-1959 and 1970-1974, *Journal of Geophysical Research*, *100*, 10,559–10,566.

Fiúza, A. F. G. (1982), The Portuguese coastal upwelling system, in *Actual problems of oceanography in Portugal, Seminar held in Lisbon on 20th and 21st November 1980, JNICT-NATO, Lisbon, 1982*, pp. 45–71.

Fiúza, A. F. G. (1983), Upwelling patterns off Portugal, in *Coastal upwelling*, edited by E. Suess and J. Thiede, pp. 85–98, Plenum.

Fiúza, A. F. G. (1984), Hidrologia e dinâmica das águas costeiras de Portugal [Hydrology and dynamics of Portuguese coastal waters], Ph.D. thesis, University of Lisbon.

Higdon, D. (2002), Space and space-time modeling using process convolutions, in *Quantitative Methods for Current Environmental Issues*, edited by C. Anderson, V. Barnett, P. C. Chatwin, and A. H. El-Shaarawi, pp. 37–56, Springer Verlag, London.

Husby, D. M, and C. S. Nelson (1982), Turbulence and vertical stability in the California Current, *CalCOFI Rep., XXIII*, 113–129.

Kennedy, V. S., R. R. Twilley, J. A. Kleypas, J. H. C. Jr., and S. R. Hare (2002), *Coastal and marine ecosystems and global climate change - potential effects on US resources*, Pew Centre on Global Climate Change, Arlington, VA.

Kern, J. (2000), Bayesian process-convolution approaches to specifying spatial dependence structure, Ph.D. thesis, Duke University.

Kifani, S. (1998), Climate dependent fluctuations of the Moroccan sardine and their impact on fisheries, in *Global versus local changes in upwelling systems*, edited by M.-H. Durand, P. Cury, R. Mendelssohn, C. Roy, A. Bakun, and D. Pauly, pp. 235–248, ORSTOM.

Kushnir, Y. (1994), Interdecadal variations in north atlantic sea surface temperature and associated atmospheric conditions, *Journal of Climate*, *7*(1), 141–157.

Lemos, R. T., and H. O. Pires (2004), The upwelling regime off the west Portuguese coast, 1941-2000, *International Journal of Climatology*, *24*(4), 511–524.

Martins, C. S., M. Hamann, and A. F. G. Fiúza (2002), Surface circulation in the eastern North Atlantic from drifters and altimetry, *Journal of Geophysical Research*, *107*(3217).

Mendelssohn, R., and F. B. Schwing (2002), Common and uncommon trends in sst and wind stress in the California and Peru-Chile Current Systems, *Progr. Oceanogr.*, *53*.

Mendelssohn, R., F. B. Schwing, and S. J. Bograd (2003), Spatial structure of subsurface temperature variability in the california current, 1950-1993, *Journal of Geophysical Research*, *108*(C3), 3093, doi:10.1029/2002JC001,568.

Mote, P. W., and N. J. Mantua (2002), Coastal upwelling in a warmer future, *Geophysical Research Letters*, *29*(23), 2138, doi: 10.1029/2002GL016,086.

Pires, H. O., and S. Antunes (2000), Climatic variability, Portuguese coastal upwelling and sardine fisheries, in *Proceedings of the 3rd European Conference on Applied Climatology, Pisa (CD-ROM)*.

Priestley, M. (1981), *Spectral Analysis and Time Series*, Academic Press, San Diego, USA.

Roy, C., and R. Mendelssohn (1998), The development and the use of a climatic database for ceos using the coads dataset, in *Global versus local changes in upwelling systems*, edited by M.-H. Durand, P. Cury, R. Mendelssohn, C. Roy, A. Bakun, and D. Pauly, pp. 27–44, ORSTOM.

Santer, B. D., T. M. L. Wigley, J. S. Boyle, D. J. Gaffen, J. J. Hnilo, D. Nychka, D. E. Parker, and K. E. Taylor (2000), Statistical significance of trends and trend differences in layer-average atmospheric temperature time series, *Journal of Geophysical Research*, *105*, 7337–7356.

Schlitzer, R. (2003), Ocean Data View, http://www.awi-bremerhaven.de/GEO/ODV.

Schwing, F. B., and R. Mendelssohn (1998), Long-term variability in the seasonality of Eastern Boundary Current (EBC) Systems: An example of increased upwelling from the California Current, in *Global versus local changes in upwelling systems*, edited by M.-H. Durand, P. Cury, R. Mendelssohn, C. Roy, A. Bakun, and D. Pauly, pp. 79–100, ORSTOM.

Schwing, F. B., R. Parrish, and R. Mendelssohn (1998), Recent trends in the spatial structure of wind forcing and SST in the California Current System, in *Global versus local changes in upwelling systems*, edited by M.-H. Durand, P. Cury, R. Mendelssohn, C. Roy, A. Bakun, and D. Pauly, pp. 101–125, ORSTOM.

Seidel, D. J., and J. R. Lanzante (2004), An assessment of three alternatives to linear trends for characterizing global atmospheric temperature changes, *Journal of Geophysical Research*, *109*(D14108), doi:10.1029/2003JD004,414.

Smyth, T. J., P. I. Miller, S. B. Groom, and S. J. Lavender (2001), Remote sensing of sea surface temperature and chlorophyll during Lagrangian experiments at the Iberian margin, *Progress in Oceanography*, *51*, 269–281.

Snyder, M. A., L. C. Sloan, N. S. Diffenbaugh, and J. L. Bell (2003), Future climate change and upwelling in the california current, *Geophysical Research Letters*, *30*(15), 1823, doi:10.1029/2003GL017,647.

Sousa, M. F. (1995), Mesoscale processes off the Portuguese coast using satellite and *in situ* observations, Ph.D. thesis, University of Lisbon.

Stephens, C., J. I. Antonov, T. P. Boyer, M. E. Conkright, R. A. Locarnini, T. D. OBrien, and H. E. Garcia (2002), *World Ocean Atlas 2001, Volume 1: Temperature.* S. Levitus, Ed., NOAA Atlas NESDIS 49, U.S. Government Printing Office, Wash., D.C., 167 pp., CD-ROMs.

Stroud, J., P. Müller, and B. Sansó (2001), Dynamic models for spatio-temporal data, *Journal of the Royal Statistical Society, B*, *63*, 673–689.

Tomé, A. R., and P. M. A. Miranda (2004), Piecewise linear fitting and trend changing points of climate parameters, *Geophysical Research Letters*, *31*(L02207).

Ventura, V., C. J. Paciorek, and J. Risbey (2004), Controlling the proportion of falsely rejected hypotheses when conducting multiple tests with climatological data, *Journal of Climate*, *17*(22), 4343–4356.

West, M., and J. Harrison (1997), *Bayesian Forecasting and Dynamic Models, 2nd ed.*, Springer Verlag, New York, USA.

Woodruff, S. D., H. F. Diaz, J. D. Elms, and S. J. Worley (1998), Coads release 2 data and metadata enhancements for improvements of marine surface flux fields, *Phys. Chem. Earth*, *23*, 517–526.

Wright, D. G., R. M. Hendry, J. W. Loder, and F. W. Dobson (1986), Oceanic changes associated with global increases in atmospheric carbon dioxide: a preliminary report for the atlantic coast of canada, *Can. Tech. Rep. Fish. Aquat. Sci.*, *1426*.

Yue, S., and S. H. Wang (2002), Regional streamflow trend detection with consideration of both temporal and spatial correlation, *Int. J. Climatol.*, *22*, 933–946.

Yue, S., P. Pilon, B. Phinney, and G. Cavadias (2002), The influence of autocorrelation on the ability to detect trend in hydrological series, *Hydrological Processes*, *16*, 1807–1829.

Ricardo T. Lemos, Faculdade de Ciências da Universidade de Lisboa, Edifício C8, 1800-100 Lisboa, Portugal. (rtl@net.sapo.pt)

Bruno Sansó, Department of Applied Mathematics and Statistics, Baskin School of Engineering, University of California, 1156 High Street MS: SOE2, Santa Cruz, CA 95064, USA. (bruno@ams.ucsc.edu)